PROCEEDINGS OF SCIENCE

TMDs and Monte Carlo Event Generators

F Hautmann*
University of Oxford / University of Antwerp
Also at: UPV/EHU, Bilbao and CERN, Geneva
E-mail: francesco.hautmann@physics.ox.ac.uk

We discuss prospects for Monte Carlo event generators incorporating the dynamics of transverse momentum dependent (TMD) parton distribution functions. We illustrate TMD evolution in the parton branching formalism, and present Monte Carlo applications of the method.

23rd International Spin Physics Symposium - SPIN2018 -
10-14 September, 2018
Ferrara, Italy

*Speaker.

PoS(SPIN2018)059

1. Introduction

Transverse momentum dependent parton distribution functions (TMD PDFs, or TMDs for short) encode nonperturbative information on hadron structure, including transverse momentum and polarization degrees of freedom, and enter QCD factorization theorems for physical observables in hadronic collisions both in the Sudakov region [1, 2] and in the high-energy region [3, 4]. They provide a "3-dimensional imaging" of hadron structure, extending to the transverse plane the 1-dimensional picture given by collinear PDFs [5].

While a great amount of knowledge has been built about collinear PDFs from experiments in hadron collisions over the past thirty years, TMDs are much less known, and hadronic 3-D imaging, with its implications for high-energy physics, will constitute the subject of intensive studies in the forthcoming decade. Experimental data analyses require realistic Monte Carlo event simulations. The construction of Monte Carlo generators incorporating TMDs is thus a central objective of this physics program.

This article describes progress in this direction based on the works [6, 7]. Sec. 2 discusses the parton branching (PB) formulation of TMD evolution. Sec. 3 presents Monte Carlo (MC) calculations using PB TMDs with applications to deep inelastic scattering (DIS) and Drell-Yan (DY) processes. Sec. 4 gives concluding remarks.

2. TMD evolution in the parton branching formalism

Table 1 gives the full set of quark (left) and gluon (right) unpolarized and polarized TMD distributions in a spin-1/2 hadron [8]. Columns represent parton polarization, rows represent hadron polarization. The f, g and h distributions on the diagonal are respectively the unpolarized, helicity and transversity TMDs. The blue and pink shades of the boxes indicate respectively T-even and T-odd distributions, i.e., involving an even or odd number of spin flips. In this article we concentrate on QCD evolution in the unpolarized case.

Although TMDs are nonperturbative quantities, QCD factorization theorems, combined with renormalization group analysis, imply that the evolution of TMDs with mass and/or energy scales can be expressed in terms of perturbative kernels, computable as power series expansions in the QCD coupling α_s. Well-known examples are provided by the CSS evolution equation (or its variants) in the Sudakov region, and BFKL evolution equation (or its variants) in the high-energy region. These achieve the resummation of logarithmically-enhanced radiative corrections (double-log in the Sudakov case, single-log in the high-energy case) to all orders in α_s, and give rise to a successful phenomenology, even though limited in each case to a specific kinematic region and a specific set of observables.

In Refs. [6, 7] a different approach from the above formalisms is proposed, which looks for a formulation of TMD evolution that can be useful in more general collider kinematics and for broader classes of observables, aiming to fulfill the following criteria: i) applicability over a wide kinematic range from low to high transverse momenta; ii) implementability in Monte Carlo event generators describing the exclusive structure of the final states; iii) evolution equations which are connected in a controllable way with DGLAP evolution equation of collinear PDFs. To this end, Refs. [6, 7] use the unitarity picture of parton evolution [9, 10] (commonly employed in parton

QUARKS	unpolarized	chiral	transverse
U	f_1		$h_1^\perp$
L		g_{1L}	$h_{1L}^\perp$
T	$f_{1T}^\perp$	g_{1T}	h_{1T}, $h_{1T}^\perp$

GLUONS	unpolarized	circular	linear
U	f_1^g		$h_1^{\perp g}$
L		g_{1L}^g	$h_{1L}^{\perp g}$
T	$f_{1T}^{\perp g}$	g_{1T}^g	h_{1T}^g, $h_{1T}^{\perp g}$

Table 1: *(left) Quark and (right) gluon TMD PDFs [8].*

shower algorithms). Soft gluon emission and transverse momentum recoils are treated by introducing the soft-gluon resolution scale to separate resolvable and non-resolvable branchings and the Sudakov form factor to express the probability for no resolvable branching in a given evolution interval. The TMD evolution equation in the parton branching (PB) approach is given by [7]

$$\mathscr{A}_a(x,\mathbf{k},\mu^2) = \Delta_a(\mu^2)\,\mathscr{A}_a(x,\mathbf{k},\mu_0^2) + \sum_b \int \frac{d^2\mathbf{q}'}{\pi\mathbf{q}'^2}\,\frac{\Delta_a(\mu^2)}{\Delta_a(\mathbf{q}'^2)}\,\Theta(\mu^2-\mathbf{q}'^2)\,\Theta(\mathbf{q}'^2-\mu_0^2) \times \int_x^{z_M}\frac{dz}{z}\,P_{ab}^{(R)}(\alpha_s,z)\,\mathscr{A}_b(x/z,\mathbf{k}+(1-z)\mathbf{q}',\mathbf{q}'^2)\ , \tag{2.1}$$

where $\mathscr{A}_a(x,\mathbf{k},\mu^2)$ is the TMD distribution of flavor a at longitudinal momentum fraction x, transverse momentum $\mathbf{k}$, evolution scale μ; z_M is the soft-gluon resolution scale; $P_{ab}^{(R)}$ are the real-emission splitting kernels, computed as a perturbative series expansion in α_s to leading order (LO), next-to-leading-order (NLO), etc.; Δ_a is the Sudakov form factor, given by

$$\Delta_a(\mu^2) = \exp\left(-\sum_b \int_{\mu_0^2}^{\mu^2}\frac{d\mu'^2}{\mu'^2}\int_0^{z_M} dz\,z\,P_{ba}^{(R)}(\alpha_s,z)\right)\ . \tag{2.2}$$

An important point in obtaining TMD distributions from the PB method concerns the ordering variables used to perform the branching evolution. The basic issue is that the transverse momentum generated radiatively by the recoils in the evolution cascade depends on the treatment of the non-resolvable region $z\to 1$ [11]. While in the collinear distribution, obtained by integration over $\mathbf{k}$, $z\to 1$ singularities cancel between real and virtual non-resolvable emissions, this is not guaranteed in the case of the TMD distribution, and supplementary conditions are needed. In the PB method these are provided by gluon emissions' angular ordering. The rescaling and shift in the transverse momentum argument of $\mathscr{A}$ in the last term on the r.h.s. of Eq. (2.1) take into account the angular ordering condition.

By integrating Eq. (2.1) over transverse momenta one obtains collinear initial-state distributions. For $z_M\to 1$, these are collinear PDFs, and one recovers DGLAP evolution equations. The convergence to DGLAP has been verified numerically in [7] at NLO to better than 1 % over several orders of magnitude in x and μ. This is in a similar spirit to the earlier studies [12, 13]. For general z_M, the evolution equation that follows from integrating Eq. (2.1) coincides with the coherent branching equation [14, 15].

The TMD branching equation (2.1) can be solved by Monte Carlo methods. Such a solution has been presented in [7]. This allows one not only to determine the inclusive distributions but also

to reconstruct exclusively the radiative final states. The principle on which the PB method is based is similar to that of parton showers, but the difference is that in the PB method nonperturbative TMD densities are defined and determined from fits to experimental data, which places constraints on fixed-scale inputs to evolution. This is in the spirit of approaches discussed e.g. in [16, 17], and is in contrast to parton shower Monte Carlo calculations, in which parton densities are not used to constrain evolution, while nonperturbative physics parameters are tuned. Monte Carlo applications of the PB method are presented in the next section for deep inelastic scattering (DIS) and Drell-Yan (DY) lepton pair production.

3. Inclusive DIS and DY p_T distribution

Applications of the PB approach to physical observables in hadronic collisions require the use of perturbative matrix elements for the production of a hard final state with high momentum transfer along with the multi-parton cascade from the TMD branching equation (2.1). The distributions $\mathscr{A}_a(x,\mathbf{k},\mu_0^2)$ in the first term on the r.h.s. of Eq. (2.1) are initial conditions which represent the intrinsic x and k_T distributions at scale μ_0, and are to be determined from fits to experiment. In this section we describe the results of determining these distributions at NLO from the high-precision inclusive DIS measurements, and using the branching equation (2.1) along with NLO perturbative matrix elements for Z-boson DY hadroproduction to obtain the PB - TMD predictions for DY transverse momentum p_T and ϕ^* spectra.

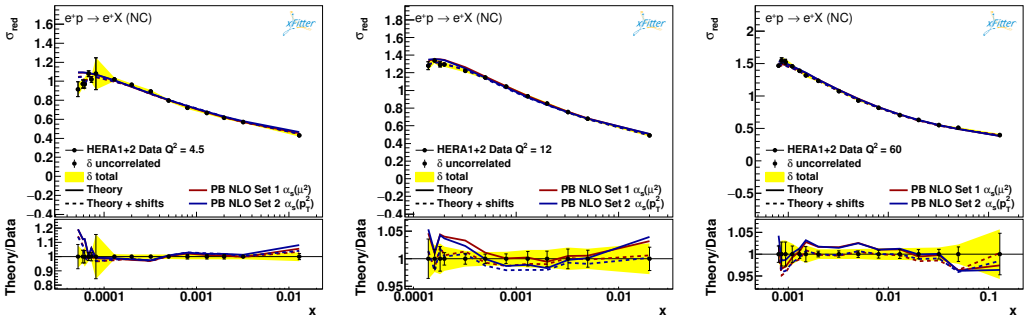

Figure 1: Measurements of the reduced cross section [19] compared to predictions using PB - TMD Set 1 and Set 2 from [18].

Figs. 1, 2 [18] show results from PB fits to the HERA high-precision inclusive DIS data [19]. The fits use NLO evolution kernels in Eq. (2.1) and NLO DIS hard-scattering coefficient functions [20]. They are performed using the open-source fitting platform `xFitter` [21] and the numerical techniques developed in [22] to treat the transverse momentum dependence in the fitting procedure. Fig. 1 illustrates the description of the reduced DIS cross section measured at HERA by the fitted TMDs. In Fig. 1 two fitted TMD sets are presented, differing by the treatment of the momentum scale in the coupling α_s, so that one can compare the effects of α_s evaluated at the transverse momentum scale prescribed by the angular-ordered branching [14, 18] with α_s evaluated at the evolution scale. The TMDs are extracted including a determination of experimental and theoretical uncertainties. An example of such results is given in Fig. 2, showing the transverse

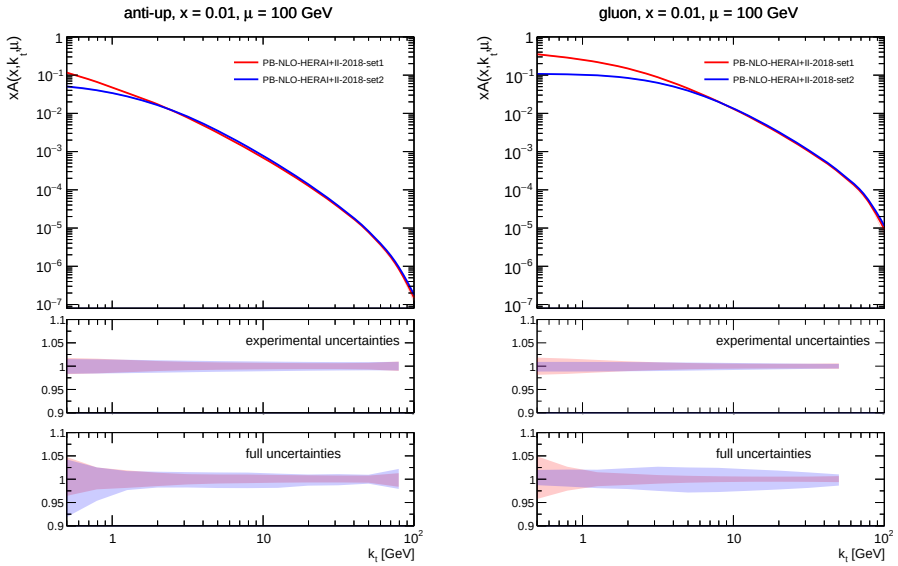

Figure 2: TMD $\bar{u}$ and gluon distributions as a function of k_T for $\mu = 100$ GeV at $x = 0.01$ [18]. In the lower panels we show the relative uncertainties coming from experimental uncertainties and the total of experimental and model uncertainties.

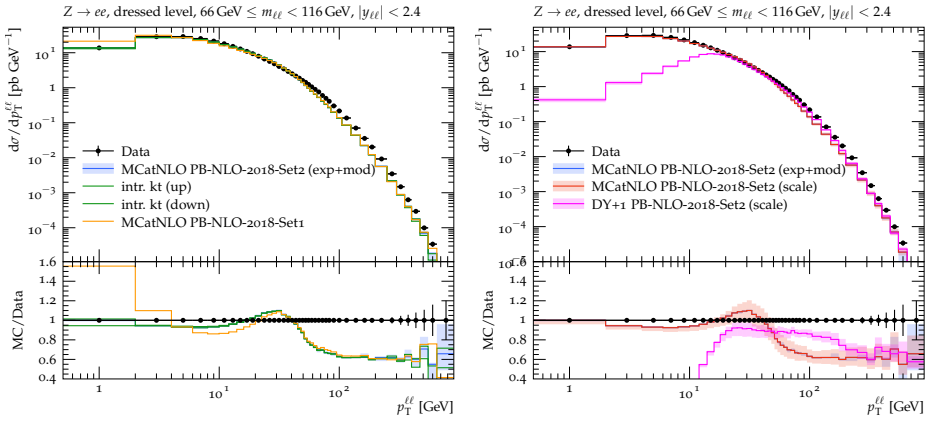

Figure 3: Transverse momentum p_T spectrum of Z -bosons as measured by [26] at $\sqrt{s} = 8$ TeV compared to the prediction [25] using aMC@NLO and NLO PB -TMD. Left: uncertainties from the PB -TMD and from changing the width of the intrinsic gaussian distribution by a factor of two. Right: with uncertainties from the TMDs and scale variation combined.

momentum dependence of $\bar{u}$ and gluon distributions for fixed values of x and μ, and associated uncertainties.

The k_T dependence in Fig. 2 results from intrinsic transverse momentum and evolution. The intrinsic k_T in Fig. 2 is described by a simple gaussian at $\mu_0 \sim \mathcal{O}$ (1 GeV) with (flavor-independent and x-independent) width $\sigma = k_0/\sqrt{2}$, $k_0 = 0.5$ GeV. This is to be compared with higher values of intrinsic $k_T \sim 2$ - 3 GeV obtained from tuning in shower MC event generators [23, 24].

In Figs. 3, 4 [25] the PB TMDs are combined with the NLO calculation of DY Z-boson pro-

duction to determine predictions for the lepton pair transverse momentum p_T spectrum and ϕ^* spectrum and compare them with LHC measurements [26]. This computation requires addressing issues of matching [27], analogous to those that arise in the case of parton showers. The matching is accomplished using the aMC@NLO framework [28], as described in [25]. The calculations are performed using CASCADE [29] to read LHE [30] files and produce output files, and RIVET [31] to analyze the outputs.

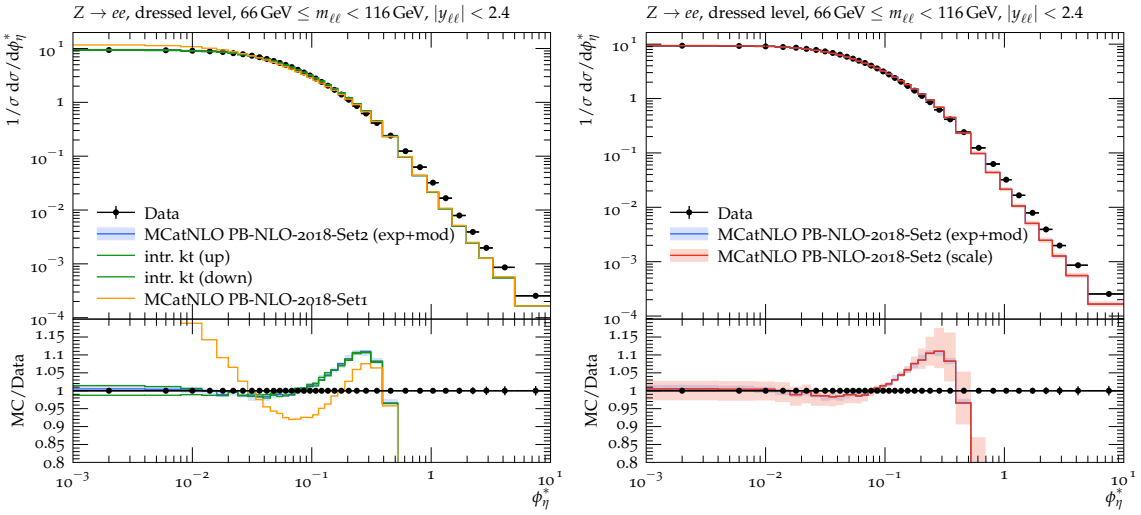

Figure 4: ϕ^* spectrum of Z -bosons as measured by [26] at $\sqrt{s} = 8$ TeV compared to the prediction [25] using aMC@NLO and NLO PB -TMD. Left: uncertainties from the PB -TMD and from changing the width of the intrinsic gaussian distribution by a factor of two. Right: with uncertainties from the TMDs and scale variation combined.

We see from the left panel in Fig. 3 that the spectrum at low p_T is sensitive to the angular ordering effects embodied in the different treatment of α_s in the PB Set 1 and Set 2. The behaviors in the DY spectrum come from the k_T distributions in Fig. 2. The uncertainties on the DY predictions in Figs. 3 and 4 come from TMD uncertainites and scale variations, with the latter dominating the overall uncertainty. The bump in the p_T distribution for intermediate p_T is an effect of the matching and the matching scale — a similar effect is seen when using parton showers instead of PB TMD. The deviation in the spectrum at higher p_T is due to including only $\mathcal{O}(\alpha_s)$ corrections but missing higher orders. We see from the right panel of Fig. 3 that the contribution from DY + 1 jet at NLO plays an important role at larger p_T.

In Fig. 5 we focus on the region of lowest transverse momenta accessible at the LHC, which is the region most sensitive to the nonperturbative and resummed QCD contributions. We show predictions from PB TMDs and from parton showers, all of which are obtained using the same aMC@NLO framework for the hard process at NLO (with appropriate subtractions terms, and the same collinear densities). While all calculations tend to agree for larger p_T, differences are observed for $p_T <$ 5 - 10 GeV. In particular, the prediction using HERWIG6, which has parameter settings that were not tuned to recent measurements, serves as an illustration of the sensitivity of MC tunes. Dedicated measurements with fine p_T binning in the region $p_T <$ 5 - 10 GeV will

allow one to investigate TMD dynamics and analyze resummation, showering and nonperturbative contributions.

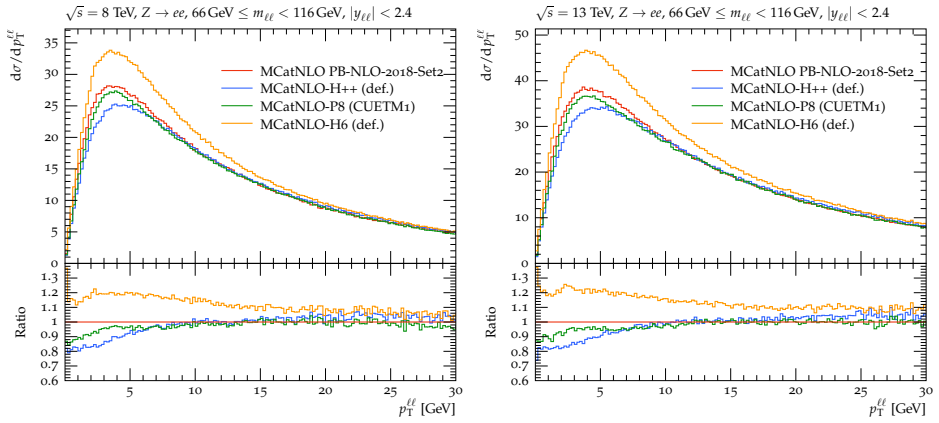

Figure 5: Transverse momentum p_T^{ll} spectrum of Z -bosons at $\sqrt{s} = 8$ TeV(left) and 13 TeV (right) obtained with the PB method [25], the parton shower of PYTHIA8 [24] with tune CUETP8M1 [32], HERWIG++ [23], and HERWIG6 [33].

4. Conclusion

MC event generators incorporating the dynamics of TMD parton distribution and fragmentation functions are instrumental in the development of high-energy physics programs which rely on precision experiments in hadron collisions at the highest luminosities or highest energies.

We have discussed TMD evolution in the parton branching formalism, and presented the TMD branching equation. This approach is designed to be implementable in MC event generators, applicable over kinematic regions ranging from low to high transverse momenta, connectible in a direct manner with DGLAP evolution of collinear distributions.

We have illustrated ongoing MC work, presenting results of matching PB TMDs with NLO calculations of DY lepton pair production via the method of aMC@NLO, and comparing the predictions thus obtained with measurements of DY p_T and ϕ^* spectra at the LHC.

The PB approach can be extended in both its nonperturbative and perturbative aspects. On one hand, non-gaussian intrinsic distributions may be taken into account, including flavor-dependence and x-dependence. This is relevant to perform PB TMD fits to experimental data for broader sets of processes and observables besides inclusive DIS.

On the other hand, the logarithmic accuracy at low transverse momenta may be improved through perturbative coefficients in the Sudakov form factor and kernel of the TMD branching equation, and the finite-order accuracy at high transverse momenta through matching with corrections of higher jet multiplicity and higher perturbative order.

We have discussed PB TMDs in the unpolarized case. The extension to polarized TMDs in Table 1 will be relevant both for experiments with polarized hadron beams and for studies of parton polarization effects, e.g. double spin flip effects for gluon fusion processes, in experiments with unpolarized hadron beams.

References

[1] J. C. Collins, *Foundations of perturbative QCD*, CUP 2011.

[2] J. C. Collins, D. E. Soper and G. Sterman, Nucl. Phys. B**250** (1985) 199.

[3] S. Catani, M. Ciafaloni and F. Hautmann, Nucl. Phys. B**366** (1991) 135.

[4] S. Catani and F. Hautmann, Nucl. Phys. B**427** (1994) 475.

[5] K. Kovařík, P. M. Nadolsky and D. E. Soper, arXiv:1905.06957 [hep-ph].

[6] F. Hautmann, H. Jung, A. Lelek, V. Radescu and R. Žlebčík, Phys. Lett. B **772** (2017) 446.

[7] F. Hautmann, H. Jung, A. Lelek, V. Radescu and R. Žlebčík, JHEP **1801** (2018) 070.

[8] R. Angeles-Martinez *et al.*, Acta Phys. Polon. B **46** (2015) 2501.

[9] B. R. Webber, Ann. Rev. Nucl. Part. Sci. **36** (1986) 253.

[10] R. K. Ellis, W. J. Stirling and B. R. Webber, *QCD and collider physics*, CUP 1996.

[11] F. Hautmann, Phys. Lett. B **655** (2007) 26.

[12] S. Jadach and M. Skrzypek, Acta Phys. Polon. B **35** (2004) 745.

[13] H. Tanaka, Prog. Theor. Phys. **110** (2003) 963.

[14] S. Catani, G. Marchesini and B. R. Webber, Nucl. Phys. B **349** (1991) 635.

[15] G. Marchesini and B. R. Webber, Nucl. Phys. B **310** (1988) 461.

[16] F. Hautmann, H. Jung, M. Krämer, P. J. Mulders, E. R. Nocera, T. C. Rogers and A. Signori, Eur. Phys. J. C **74** (2014) 3220.

[17] J. C. Collins and T. C. Rogers, Phys. Rev. D 91 (2015) 074020.

[18] A. Bermudez Martinez *et al.*, Phys. Rev. D 99 (2019) 074008; arXiv:1809.04511 [hep-ph].

[19] ZEUS, H1 Collaboration, Eur. Phys. J. C75 (2015) 580.

[20] M. Botje, Comput. Phys. Commun. **182** (2011) 490.

[21] S. Alekhin *et al.*, Eur. Phys. J. C **75** (2015) 304.

[22] F. Hautmann, H. Jung and S. Taheri Monfared, Eur. Phys. J. C **74** (2014) 3082.

[23] M. Bahr *et al.*, Eur. Phys. J. C **58** (2008) 639.

[24] T. Sjöstrand *et al.*, Comput. Phys. Commun. 191 (2015) 159.

[25] A. Bermudez Martinez *et al.*, arXiv:1906.00919 [hep-ph].

[26] ATLAS Collaboration, Eur. Phys. J. C76 (2016) 291.

[27] J. C. Collins and F. Hautmann, JHEP **0103** (2001) 016.

[28] J. Alwall *et al.*, JHEP **1408** (2014) 166.

[29] H. Jung *et al.*, Eur. Phys. J. C **70** (2010) 1237.

[30] J. Alwall *et al.*, Comput. Phys. Commun. **176** (2007) 300.

[31] A. Buckley *et al.*, Comput. Phys. Commun. **184** (2013) 2803.

[32] V. Khachatryan *et al.* [CMS Collaboration], Eur. Phys. J. C **76** (2016) 155.

[33] G. Corcella, I. G. Knowles, G. Marchesini, S. Moretti, K. Odagiri, P. Richardson, M. H. Seymour and B. R. Webber, hep-ph/0210213.